Chapter 6

Measurement and Prediction of Road Traffic Noise at Different Floor Levels of Buildings in a Mid-size Indian City

6.1 General

This study aims to unveil crucial insights into the dynamic fluctuations of noise levels within the vertical dimensions of high-rise buildings nestled amidst the bustling streets of mid-sized Indian cities where heterogeneous traffic is under operation. Two cycles of data were collected on all floors for hourly duration on the façade line for two high-rise buildings. Traffic volume, speed, distance of the building from centre of the carriageway and honking data were used to develop models for L_{eq} and L_{10} using Artificial Neural Network (ANN). This work has the novelty of addressing the impact of heterogeneous traffic noise at various floor levels of Varanasi mid-sized city which has narrow carriageway. Such a traffic has prominence of honking which is modelled perhaps for the first time. The outcome of this research has importance in urban planning and formulating legislations.

6.2 Road Traffic Information

Building – 1 (25°21'50.2"N 83°01'58.4"E) was adjacent to the Ashapur road on Varanasi-Ghazipur National highway, whereas building – 2 (25°18'22.5"N 82°59'10.6"E) was along the Mahmoorganj-Sigra road. Traffic was categorised into 2-wheeler (2-w), 3-wheeler (3-w), car, Light Commercial Vehicle (LCV), Tractor, Bus, Truck, rickshaw (tricycle), e-rickshaw (battery-driven tricycle) and bi-cycle. Figure 6.1 shows that 2-w have a disproportionately

large share of traffic on both roads. It ranges between 53-69% for Ashapur road and 63- 75% for Mahmoorganj-Sigra road. For Ashapur road, the volume of 3-w, car, LCV, e-rickshaw, and rickshaw varied between 5-14%, 9-20%, 1-5%, and <1%, respectively. Heavy vehicles like trucks were less than 1%, while buses ranged between 0-3%. On Mahmoorganj-Sigra road 3-w, cars, LCVs, e-rickshaws, and rickshaws ranged from 2-8%, 5-12%, 1-4%, 4-10%, and <1%, respectively. Heavy vehicles (bus and truck) accounted for less than 1% of the traffic volume.

The non-motorized vehicle also contributed significantly to the traffic of both locations. Bi-cycle ranged between 5-17% for Ashapur road, while for Mahmoorganj-Sigra road, it was between 3-12%. As can be seen from Table 6.3, the overall traffic volume every 15 minutes on the Mahmoorganj-Sigra road was higher than that on the Ashapur road. Honking counts on Mahmoorganj-Sigra road were also more significant than on Ashapur road. The carriageway width of Ashapur road was 10m (double-lane two-way) while that of Mahmoorganj-Sigra road was 17m (four–lane divided carriageway). The surface type of Ashapur road was concrete, while that of Mahmoorganj- Sigra road was bituminous. The road had a grade of less than 2%.

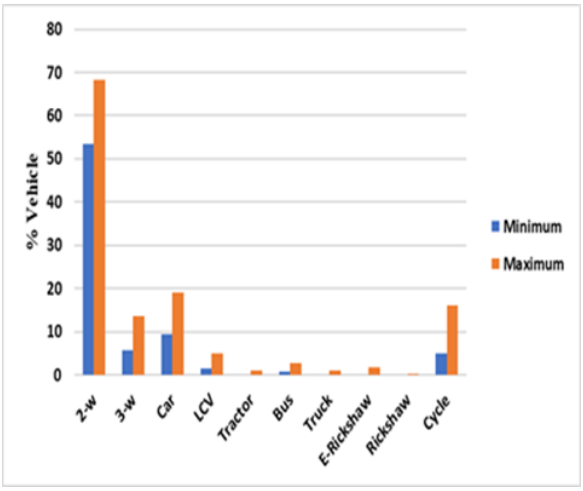

a) Building 1. Besides Ashapur road

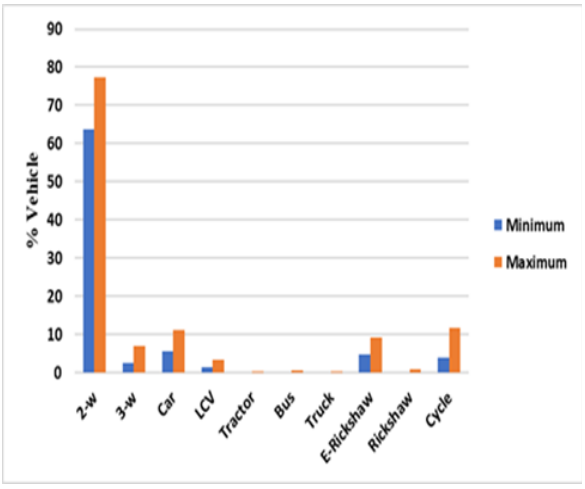

b) Building 2. Besides Mahmoorganj - Sigra road

Figure 6.1. Classified traffic volume at data collection site

6.3 Result and Analysis for Vertical Noise Propagation

6.3.1 Noise level variation across for heights

The roadside noise level for Ashapur road and Mahmoorganj-Sigra road ranged between 77-80 dB(A) and 78-81 dB(A), respectively. Figure 6.2 shows that in building 1, noise level ($L_{\mathrm{Aeq,1h}}$) between floors fluctuated between 66 and 73 dB(A) during cycle 1 and between 64 and 72 dB(A) during cycle 2. Figure 6.3 shows that in building 2, the range for $L_{\mathrm{Aeq,1h}}$ was 69-74 dB(A) for both cycles. The L_{10} noise level varied between 66-73 dB(A) and 72-77 dB(A) for both the cycles of building 1 and building 2, respectively. According to World health Organisation the L_{Aeq} for outdoor living area should not exceed 50-55 dB(A). In both buildings at different floor levels, the background noise (L_{90}) surpassed 55 dB(A). Figure 6.4 (a) shows that building 2 was more susceptible to road noise than building 1 because of its closer location with busy road and higher hourly traffic volumes and honking counts. Both

cycles of data reveal that the noise level increase up to certain height and then decreases as it is shown in Figure 6.4(a). For building 1 (cycle 1 and cycle 2) and building 2 (cycle 2), the noise level peaked at the 3rd floor and then decreased. For building 2 (cycle 1), the noise level increased to peak at the 6th floor and then reduced. Also, the difference in noise level between the 6th and 3rd floor of building 2 (cycle 1) is 0.7 dB(A), which is insignificant. Thus, the 3rd floor may be reckoned as the floor with maximum noise level and considered as the reference floor for further analysis.

The difference in noise levels between the reference floor and all other floors facilitates the identification of the noisiest and quietest floors. From the Figure 6.4(b), it was observed that for building 1- cycle 2 (B1-C2), floor levels 2 and 4 have a difference < 1dB(A). For building 2 – cycle 1 (B2-C1), floor levels 4, 5, 6, 7, 8 and 9 and for building 2-cycle 2 (B2-C2), floor levels 4, 5 and 6 have a difference < 1dB(A). For the building 1-cycle 1 (B1-C1), there is no floor having difference < 1dB(A). Floor 4 is common among 3 cycles, and floors 5 and 6 were common among 2 cycles. From this we may conclude that floor levels 3, 4, 5 and 6 (height approx. 8.4–21 meters) were among the noisiest floors. For building 1, for both the cycles of data taken; the maximum difference of > 6 dB(A) was observed for floor level 1 and difference of 5-6 dB(A) was observed for floor level 15. For building 2, the maximum difference of 2.5-4.0 dB(A) was found on the 15th floor for both cycles. On the first floor of building 2, the difference was 2.6 dB(A). Thus, at floor level 1 and floor level above 10 of each building at each cycle, the difference seems significant and lies in the range of 2-5.8 dB(A). Thus, these floors seem to be quieter than other floor levels.

The Traffic Noise Index (TNI) was derived based on data reflecting traffic noise levels at different distances from the source, typically measured at building facades. This index is

carefully weighted to consider fluctuations in traffic flow and is strongly correlated with overall dissatisfaction levels [242]. While noise climate refers to the range within which sound levels fluctuate over a specific period of time [243]. The TNI value fluctuates from 63-73 1dB(A) for building 1 with mean value of 67.6 dB(A) and 69-86 dB(A) for building 2 with mean value of 78.43. NC varies from 8- 10.5 dB(A) for building 1 with mean value of 9.3 dB(A) and 8-13 dB(A) for building 2 with mean value of 11.18 dB(A). The TNI and NC values for different floor is shown in Table 6.1.

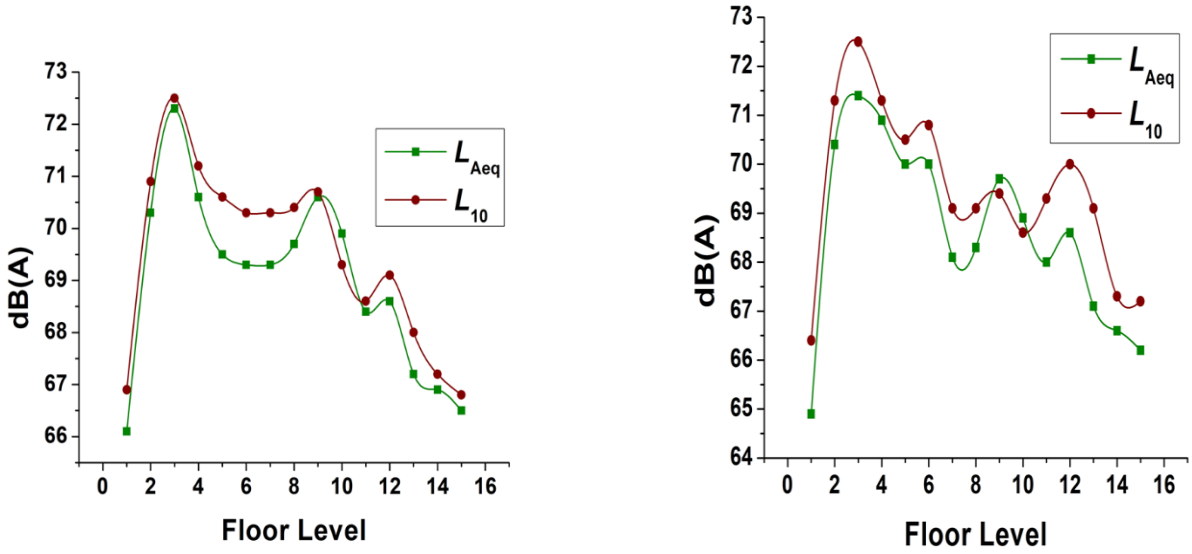

a) Cycle 1 b) Cycle 2

Figure 6.2. Noise level variation for Building 1

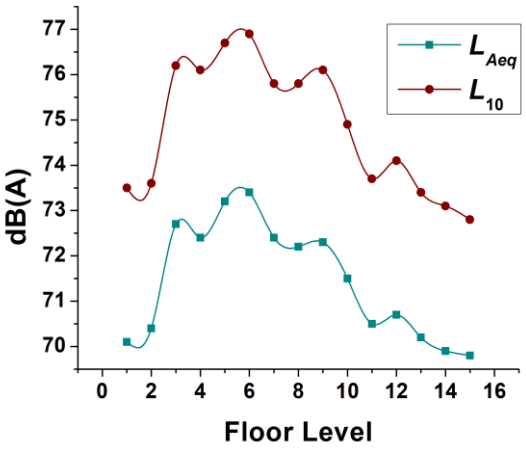

c) Cycle 1

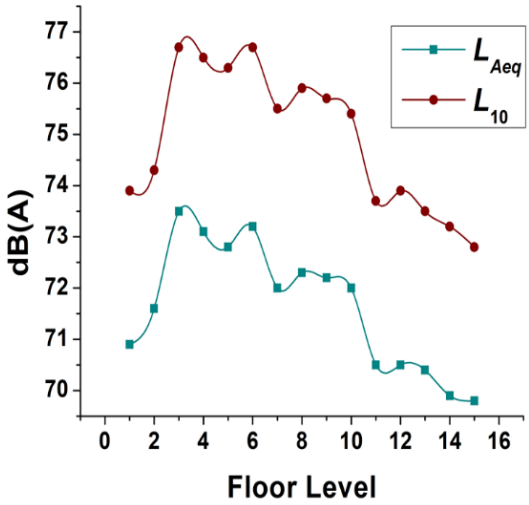

d) Cycle 2

Figure 6.3. Noise level variation for Building 2

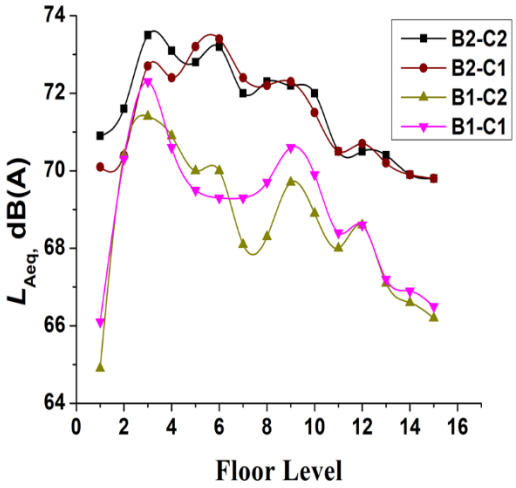

a) Overall noise variation

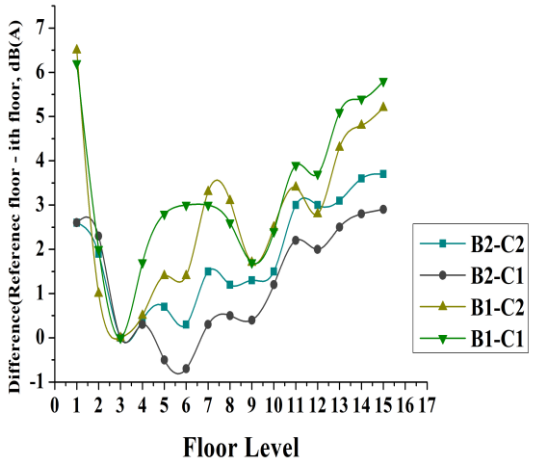

b) Difference of noise level

Figure 6.4. Analysis of noise level

Table 6.1. TNI and NC indices level at different floor of buildings

Floor ID	TNI, dB(A)				NC, dB(A)			
	B1-C1	B1-C2	B2-C1	B2-C2	B1-C1	B1-C2	B2-C1	B2-C2
1	63.3	64.3	78.6	74.2	8.8	9.3	11.7	10.1
2	68.5	71.3	78.7	75.5	9.2	10	11.7	10.4
3	69.5	72.2	82.8	80	9	9.9	12.2	11.1
4	69.1	70.7	82.7	79.8	9.3	9.8	12.2	11.1
5	68.5	69.9	85.1	83.8	9.3	9.8	12.8	12.5
6	67.3	70.5	83.8	83.6	9	9.9	12.3	12.3
7	70.3	68.5	80.9	80.6	10	9.8	11.7	11.7
8	70.1	67.9	81.8	82.5	9.9	9.6	12	12.2
9	71	68.5	82.7	82.6	10.1	9.7	12.2	12.3
10	69	68	77	80.5	9.9	9.8	10.7	11.7
11	64.4	66	74.3	75.5	8.6	8.9	10.2	10.6
12	64.9	67.3	76.5	77.2	8.6	9.1	10.8	11.1
13	63.2	66.4	73.1	72.3	8.4	9.1	9.9	9.6
14	65.1	64.3	73.7	73.2	9.3	9	10.2	10
15	63.8	64.2	70.4	69.5	9	9	9.2	8.9

6.3.2 Frequency analysis

Figure 6.5 depicts the A-weighted noise level across different frequencies within one-third octave bands at various floor levels. Figure 6.5(a) and Figure 6.5(b) shows that most of the energy on each floor of building 1 was caused by low-frequency noise, and the dominating frequency (DF) was also found to be in the low-frequency range as shown in Figure 6.6(a) and Figure 6.6(b) which is attributable to operation of traffic as discussed in the literature. Low-frequency sound is sometimes defined as having a frequency lower than 250 Hz, even though some people have decided to cap the range at a maximum of 100 Hz [256]. In building 2 also most of the noise energy is contributed from low frequency range as shown in Figure 6.5(c) and Figure 6.5(d). The dominating frequency for most of the floor levels in building 2 was in the high-frequency range as shown in Figure 6.6(c) and Figure 6.6(d). The noise level corresponding to dominant frequency are given in Table 6.2.

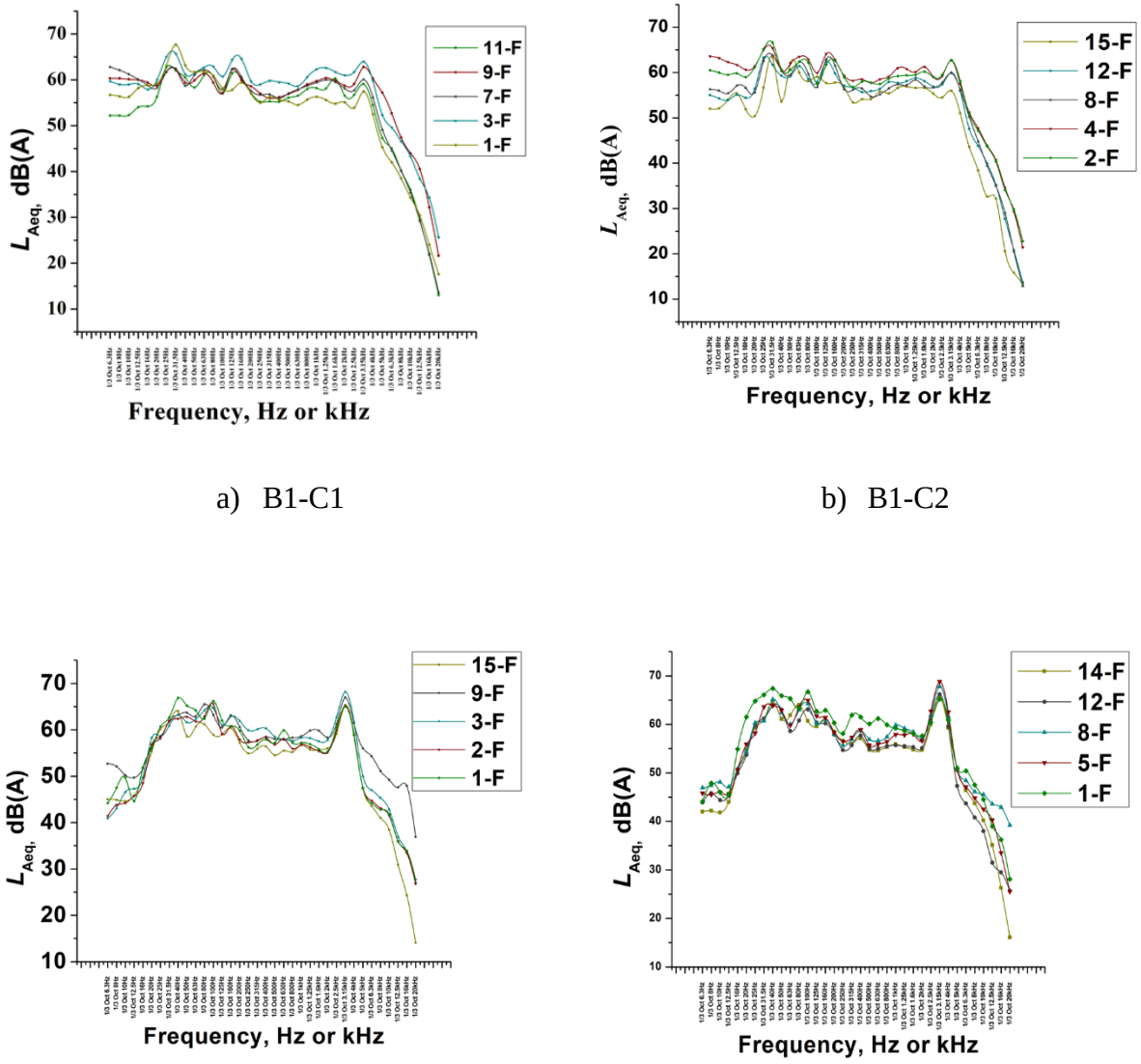

a) B1-C1

b) B1-C2

c) B2-C1

d) B2-C2

Figure 6.5. Frequency spectrum curve

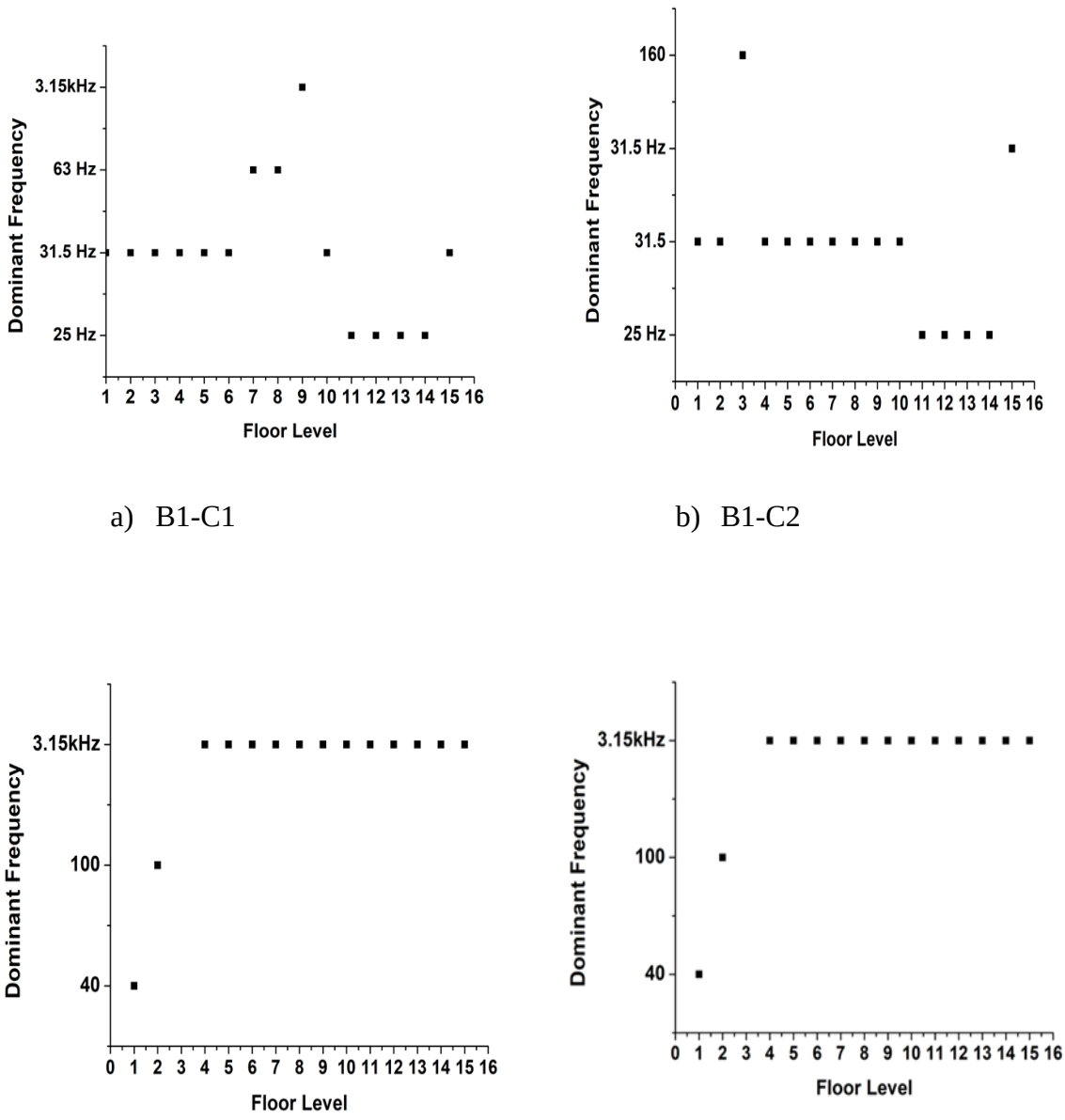

a) B1-C1

b) B1-C2

c) B2-C1

d) B2-C2

Figure 6.6. Floor wise location of dominating frequency

.

Table 6.2. Noise level corresponding to dominating frequency

Floor ID	DF: B1-C1	dB(A)	DF: B1-C2	dB(A)	DF: B2-C1	dB(A)	DF: B2-C2	dB(A)
1	31.5 Hz	67.7	31.5 Hz	67	40 Hz	66.9	40 Hz	67.4
2	31.5 Hz	66.9	31.5 Hz	66.6	100 Hz	65.6	100 Hz	65.9
3	31.5 Hz	65.7	160 Hz	64.2	3.15kHz	68.2	3.15kHz	68.6
4	31.5 Hz	65.6	31.5 Hz	65.4	3.15kHz	68.1	3.15kHz	68.4
5	31.5 Hz	65.4	31.5 Hz	65.8	3.15kHz	69	3.15kHz	68.8
6	31.5 Hz	65.3	31.5 Hz	65.7	3.15kHz	69.1	3.15kHz	69.1
7	63 Hz	62.8	31.5 Hz	62.7	3.15kHz	68	3.15kHz	67.9
8	63Hz	63.7	31.5 Hz	63.8	3.15kHz	67.9	3.15kHz	67.8
9	3.15kHz	62.8	31.5 Hz	62.7	3.15kHz	67	3.15kHz	67.6
10	31.5 Hz	62.9	31.5 Hz	63.6	3.15kHz	66.7	3.15kHz	67.6
11	25 Hz	62.7	25 Hz	62.7	3.15kHz	65.7	3.15kHz	66.3
12	25 Hz	63.5	25 Hz	63.3	3.15kHz	65.9	3.15kHz	66.2
13	25 Hz	62.3	25 Hz	61.9	3.15kHz	65.7	3.15kHz	66.1
14	25 Hz	62.9	25 Hz	63.4	3.15kHz	65.2	3.15kHz	65.5
15	31.5 Hz	63	31.5 Hz	63.4	3.15kHz	65.2	3.15kHz	65.3

DF – Dominating frequency; B1-C1 – Building 1-cycle 1; B2-C2 – Building 2- cycle 2

6.4 Result and Analysis of Traffic Noise Modeling for High rise Residential buildings

6.4.1 Descriptive statistics

Descriptive statistics of traffic volume, speed and noise level are shown in Table 6.3.

Table 6.3. Descriptive statistics

	Building 1 (Ashapur road)				**Building 2 (Mahmoorganj - Sigra road)**			
Traffic volume, vehicles/hour								
	N	Minimum	Maximum	Std. Deviation	N	Minimum	Maximum	Std. Deviation
2-w	131	287	523	57.87	127	702	1101	107.36
3-w	131	43	86	11.97	127	28	78	10.06
Car	131	43	129	15.41	127	68	123	12.36
LCV	131	10	33	4.45	127	18	42	5.049
Tractor	131	0	7	1.52	127	0	4	0.90
Bus	131	6	16	2.47	127	0	5	1.23
Truck	131	0	7	1.42	127	0	4	1.20
e-Rickshaw	131	0	10	2.69	127	59	118	15.54
Rickshaw	131	0	1	0.29	127	0	10	2.66
Bi-Cycle	131	29	142	18.44	127	46	129	20.37
Total volume	131	462	886	76.53	127	1035	1475	106.56
Traffic speed, Km/h								
2-w	131	27	39	2.83	127	18	30	2.76
3-w	131	23	36	3.14	127	16	29	2.38
Car	131	27	44	3.35	127	16	29	3.21
LCV	131	18	41	3.93	127	18	28	2.49
Tractor	131	0	31	6.00	127	0	20	9.39
Bus	131	21	44	4.60	127	0	28	10.92
Truck	131	0	33	10.27	127	0	26	10.56

e-Rickshaw	131	0	26	6.18	127	14	22	2.02
Rickshaw	131	0	15	2.95	127	0	13	2.06
Bi-Cycle	131	11	17	1.30	127	10	17	1.74
Noise level, dB(A) and honking event								
L_{eq}	131	62.9	73.8	2.3628	127	69.4	74.2	1.28
L_{max}	131	80.5	98.5	3.8409	127	79.8	93.9	3.37
L90	131	56.3	64.2	1.6928	127	61.6	66.4	0.87
L10	131	64.8	73.4	1.9888	127	72.6	78.4	1.43
Honking event	131	13	49	5.959	127	35	75	8.94

6.4.2 ANN Model Development

A total 15 number of inputs were taken to predict L_{eq} and L_{10} separately. Input parameters for the model were chosen using a combination of a review of prior research efforts and a correlation analysis conducted for the current research study. Parameters with significant correlation coefficients were used as inputs in the model-building process. The input variables were Q1 = 2 -wheeler (2-w) Volume, Q2 = 3 -wheeler (3-w) volume, Q3= Light Commercial vehicle (LCV) volume, Q4 = Bus Volume, Q5=E-Rickshaw volume, Q6 =Rickshaw Volume, Q7= Bi-cycle Volume, V1= 2-wheeler speed, V2= 3-wheeler speed, V3= Car Speed, V4 = LCV speed V5= Bus Speed, V6= Rickshaw Speed, Hypotenuse distance from centre (HD) of road to SLM microphone, Honking events (HE). Q is Vehicle volume per 15 minutes, and V is Vehicle speed in Km/h For Modeling purpose, we have divided the 1-hour data in 4 cycles of 15 minutes data. Total 131 data set in Building 1 and 127 in Building 2 were collected; each data set cycle consisted of 15 minutes. At first, the entire dataset was arbitrarily split into a training set and a test set. Eighty percent of the complete datasets were used for model training, while the remaining twenty percent were used for model testing. Models were

developed using code for an ANN technique implemented in Python (Version 3.7.9). Iteratively testing several configurations of the algorithm's code—including different numbers of hidden layers, hidden-layer neuron densities, activation functions for the hidden and output layers, and training algorithms—led to the optimal model's performance. The ANN architecture for the selected model for L_{Aeq} and L_{10} were 15-7-1 and 15-5-1 respectively. The architecture for the specified model is shown in Figure 6.7. The activation functions employed were hyperbolic tangent for the hidden layer and sigmoid for the output layer for both the selected models. Broyden–Fletcher–Goldfarb–Shanno (BFGS) training algorithms were utilized in these models. The best-fitted model was identified using numerous performance measurement parameters such as coefficient of determination (R^2), coefficient of correlation (R), mean absolute error (MAE), and root mean square error (RMSE), which are formulated through Equation (3.3) to (3.6). To enhance the network working efficiency and learning process, the input and output data were normalized between 0 and 1 using Equation (3. *2*). Inputs to this ANN model were normalised values of variables such as traffic volume, speed, hypotenuse distance, and honking Events. N in input denotes Normalised, Q denotes Traffic volume, and V represents Speed in Figure 6.7. The input and output variables information were given in section "ANN model development". According to ANN, the most fundamental mathematical equation connecting the input and output variables is represented as Equation (6.1).

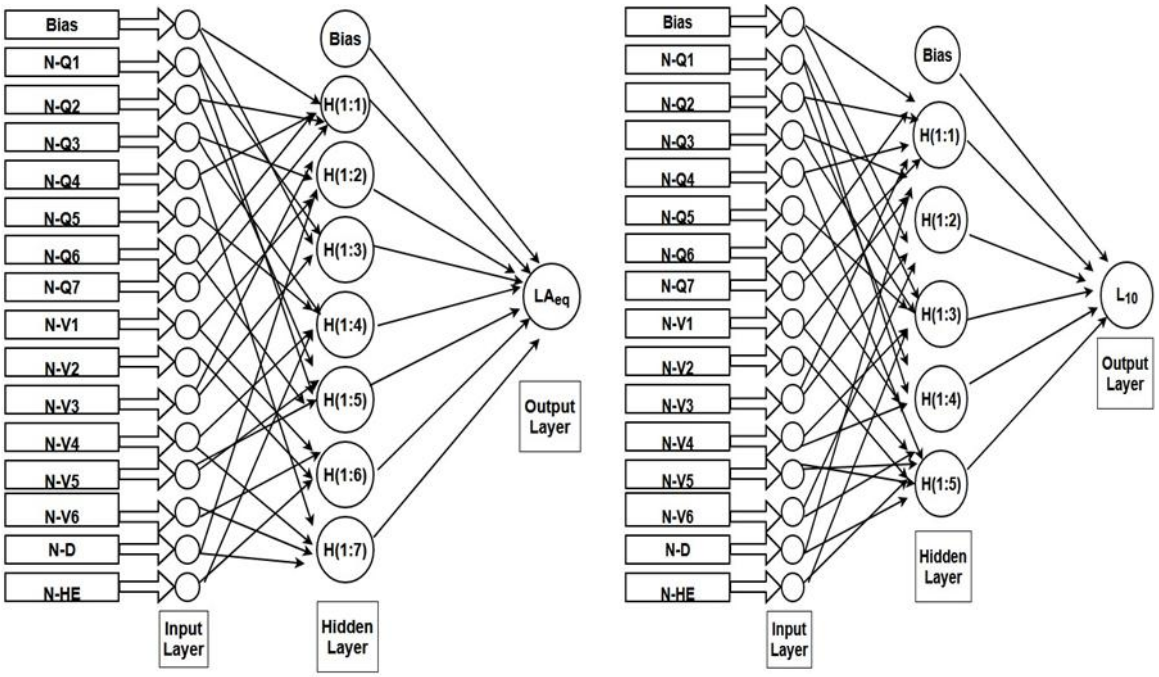

a) L_{eq} model b) L_{10} model

Figure 6.7. ANN architecture

$$Output = a_o \left[b_o + \sum_{k=1}^{h} \left\{ D_k a_h \left(b_{hk} + \sum_{i=1}^{n} D_{ik} C_i \right) \right\} \right] \tag{6.1}$$

Term a_o and a_h denotes the transfer function of output and hidden layer respectively; b_o denotes bias at output layer; D_k represents connection weight between kth neuron of hidden layer and single output neuron; b_{hk} represents bias at the kth neuron of hidden layer; h represents the number of neurons in the hidden layer; D_{ik} represents connection weight between the ith input layer and the kth neuron of the hidden layer; Ci represents input parameter.

6.4.3 Prediction equation for L_{eq}

The obtained equation for predicting the L_{eq} from ANN is shown below:

$$X1 = 2.71185 * 2_W\,(V) - 4.96095 * 3_W\,(V) + 2.92081 * LCV(V) + 0.32602 * BUS(V) + 0.41016 * E_{Rickshaw}\,(V) + 1.26199 * Rickshaw\,(V) + 0.29016 * Cycle(V) - 0.01804 * 2_W\,(S) - 0.22523 * 3_W\,(S) - 2.64657 * Car(S) - 0.49839 * LCV(S) + 0.23843 * Bus(S) + 1.09327 * Rickshaw\,(S) - 2.49472 * H_{SLM} - 2.8972 * HE - 0.10753$$

$$X2 = -2.85761 * 2_W\,(V) + 3.76735 * 3_W\,(V) + 1.71762 * LCV(V) - 7.4928 * BUS(V) - 0.80168 * E_{Rickshaw}\,(V) - 3.10237 * Rickshaw\,(V) + 2.21832 * Cycle(V) - 0.40242 * 2_W\,(S) + 1.69076 * 3_W\,(S) - 2.03025 * Car(S) - 1.73244 * LCV(S) + 0.49288 * Bus(S) + 1.20732 * Rickshaw\,(S) + 7.46033 * H_{SLM} + 0.58937 * HE - 2.74403$$

$$X3 = 6.77563 * 2_W\,(V) - 3.66953 * 3_W\,(V) - 0.02429 * LCV(V) + 1.38184 * BUS(V) + 0.45432 * E_{Rickshaw}\,(V) + 2.5703 * Rickshaw\,(V) + 0.60173 * Cycle(V) - 2.62445 * 2_W\,(S) - 1.39512 * 3_W\,(S) + 0.16308 * Car(S) + 0.83899 * LCV(S) + 0.6789 * Bus(S) - 0.03702 * Rickshaw\,(S) - 4.98893 * H_{SLM} - 2.53912 * HE - 1.68779$$

$$X4 = -1.21533 * 2_W\,(V) + 0.4281 * 3_W\,(V) + 2.7031 * LCV(V) - 0.89672 * BUS(V) - 2.38018 * E_{Rickshaw}\,(V) + 1.46096 * Rickshaw\,(V) + 2.82524 * Cycle(V) - 0.75892 * 2_W\,(S) - 2.55884 * 3_W\,(S) - 0.75737 * Car(S) + 0.67856 * LCV(S) - 0.96705 * Bus(S) - 2.05981 * Rickshaw\,(S) + 4.27285 * H_{SLM} - 5.6622 * HE + 0.56891$$

$$X5 = -0.94232 * 2_W\ (V) - 2.24902 * 3_W\ (V) - 4.17279 * LCV(V) + 1.61164 * BUS(V) - 1.86732 * E_{Rickshaw}\ (V) - 0.91888 * Rickshaw\ (V) + 0.04661 * Cycle(V) - 0.3328 * 2_W\ (S) + 0.39235 * 3_W\ (S) - 0.1515 * Car(S) - 0.60734 * LCV(S) + 0.92872 * Bus(S) - 0.72686 * Rickshaw\ (S) + 1.60228 * H_{SLM} - 0.95589 * HE - 0.75287$$

$$X6 = 7.80016 * 2_W\ (V) - 3.7863 * 3_W\ (V) + 1.75166 * LCV(V) + 1.11603 * BUS(V) + 2.06353 * E_{Rickshaw}\ (V) + 3.00311 * Rickshaw\ (V) + 3.75136 * Cycle(V) + 0.76129 * 2_W\ (S) + 0.09435 * 3_W\ (S) - 2.60339 * Car(S) + 1.24444 * LCV(S) - 2.21826 * Bus(S) - 0.18274 * Rickshaw\ (S) + 0.02767 * H_{SLM} + 4.03921 * HE - 0.59968$$

$$X7 = -0.17637 * 2_W\ (V) + 1.60199 * 3_W\ (V) - 1.84445 * LCV(V) - 0.66857 * BUS(V) - 1.20177 * E_{Rickshaw}\ (V) + 0.55009 * Rickshaw\ (V) - 2.12616 * Cycle(V) + 0.16545 * 2_W\ (S) - 0.60218 * 3_W\ (S) + 1.24711 * Car(S) + 0.82209 * LCV(S) - 0.77336 * Bus(S) + 1.05861 * Rickshaw\ (S) - 0.98752 * H_{SLM} + 1.31077 * HE - 0.2338$$

$$Y = 0.30315 + 2.27999\frac{(e^{X_1} - e^{-X_1})}{(e^{X_1} + e^{-X_1})} - 1.50292\frac{(e^{X_2} - e^{-X_2})}{(e^{X_2} + e^{-X_2})} - 2.97749\frac{(e^{X_3} - e^{-X_3})}{(e^{X_3} + e^{-X_3})} + 1.18516\frac{(e^{X_4} - e^{-X_4})}{(e^{X_4} + e^{-X_4})} - 1.19041\frac{(e^{X_5} - e^{-X_5})}{(e^{X_5} + e^{-X_5})} + 1.90485\frac{(e^{X_6} - e^{-X_6})}{(e^{X_6} + e^{-X_6})} + 1.83655\frac{(e^{X_7} - e^{-X_7})}{(e^{X_7} + e^{-X_7})}$$

$$L_{eq} = L_{eq_{Min}} + \frac{1}{(1+e^{-Y})}\left(L_{eq_{Max}} - L_{eq_{Min}}\right) \quad (6.2)$$

6.4.4 Prediction equation for L_{10}

The obtained equation for predicting the L_{10} from ANN is shown in equation:

$$\begin{aligned} R1 = {} & -0.35011 * 2_W\,(V) + 0.04273 * 3_W\,(V) - 0.36567 * LCV(V) - 0.32746 \\ & * BUS(V) - 0.41049 * E_{Rickshaw}\,(V) - 0.31623 * Rickshaw\,(V) \\ & - 0.38507 * Cycle(V) - 0.1312 * 2_W\,(S) + 0.05019 * 3_W\,(S) - 0.04165 \\ & * Car(S) - 0.03968 * LCV(S) + 0.17592 * Bus(S) - 0.25261 \\ & * Rickshaw\,(S) + 1.28801 * H_{SLM} - 0.82646 * HE - 0.57238 \end{aligned}$$

$$\begin{aligned} R2 = {} & 0.01658 * 2_W\,(V) + 0.30092 * 3_W\,(V) - 0.23588 * LCV(V) - 0.55819 * BUS(V) \\ & + 0.2014 * E_{Rickshaw}\,(V) - 0.24146 * Rickshaw\,(V) + 0.23231 \\ & * Cycle(V) - 0.40005 * 2_W\,(S) - 0.14184 * 3_W\,(S) - 0.1728 * Car(S) \\ & - 0.18001 * LCV(S) + 0.00325 * Bus(S) + 0.16807 * Rickshaw\,(S) \\ & + 1.45495 * H_{SLM} - 0.42559 * HE - 0.45691 \end{aligned}$$

$$\begin{aligned} R3 = {} & 0.03971 * 2_W\,(V) - 0.23152 * 3_W\,(V) + 0.09551 * LCV(V) + 0.20182 * BUS(V) \\ & - 0.0761 * E_{Rickshaw}\,(V) + 0.25135 * Rickshaw\,(V) - 0.29741 \\ & * Cycle(V) + 0.10011 * 2_W\,(S) - 0.09689 * 3_W\,(S) - 0.05034 * Car(S) \\ & - 0.01697 * LCV(S) - 0.2332 * Bus(S) + 0.00309 * Rickshaw\,(S) \\ & - 0.93807 * H_{SLM} + 0.30604 * HE + 0.11149 \end{aligned}$$

$$R4 = 0.34065 * 2_W\ (V) + 0.46308 * 3_W\ (V) + 0.0515 * LCV(V) - 0.27163 * BUS(V) + 0.3792 * E_{Rickshaw}\ (V) + 0.07869 * Rickshaw\ (V) + 0.35007 * Cycle(V) + 0.07928 * 2_W\ (S) + 0.04518 * 3_W\ (S) + 0.0335 * Car(S) - 0.03284 * LCV(S) + 0.32437 * Bus(S) + 0.30835 * Rickshaw\ (S) + 0.95917 * H_{SLM} + 0.00129 * HE + 0.30335$$

$$R5 = -0.63026 * 2_W\ (V) + 0.03225 * 3_W\ (V) - 0.31695 * LCV(V) - 0.26704 * BUS(V) - 0.83832 * E_{Rickshaw}\ (V) - 0.45052 * Rickshaw\ (V) - 0.84769 * Cycle(V) + 0.16618 * 2_W\ (S) + 0.25839 * 3_W\ (S) + 0.1529 * Car(S) + 0.20679 * LCV(S) + 0.27908 * Bus(S) - 0.51551 * Rickshaw\ (S) + 1.30851 * H_{SLM} - 1.11974 * HE - 0.46783$$

$$T = 0.24619 - 0.5948\frac{(e^{R_1} - e^{-R_1})}{(e^{R_1} + e^{-R_1})} - 0.59176\frac{(e^{R_2} - e^{-R_2})}{(e^{R_2} + e^{-R_2})} + 0.54098\frac{(e^{R_3} - e^{-R_3})}{(e^{R_3} + e^{-R_3})} - 0.75641\frac{(e^{R_4} - e^{-R_4})}{(e^{R_4} + e^{-R_4})} - 0.9246\frac{(e^{R_5} - e^{-R_5})}{(e^{R_5} + e^{-R_5})}$$

$$L_{10} = L_{10_{Min}} + \frac{1}{(1 + e^{-T})}\left(L_{10_{Max}} - L_{10_{Min}}\right) \quad (6.\ 3)$$

6.4.5 Model performance

Figure 6.8 to Figure 6.11 depicts the relationship between the observed and predicted noise in the training (TR) and testing (TS) data sets for L_{eq} and L_{10}, respectively. Table 6.4 shows that R^2 obtained for L_{eq} for TR and TS datasets were 0.93 and 0.84, respectively. For

predicting the L_{10}, the developed model has R^2 value of 0.90 for both TR and TS datasets. This is indicative of a high degree of agreement between the observed and projected values at various floor levels. The MAE and RMSE for L_{eq} for TR datasets are lower among various datasets followed by TS datasets of L_{eq}. The highest explained variability and lowest error achieved in the L_{eq} datasets reveal that the maximum reliable prediction can be made for L_{eq} in comparison to L_{10}. However, the overall result showed that the developed models efficiently predict the L_{eq} and L_{10} at a different floor levels of the high-rise residential buildings located close to narrow carriageway under heterogeneous traffic flow.

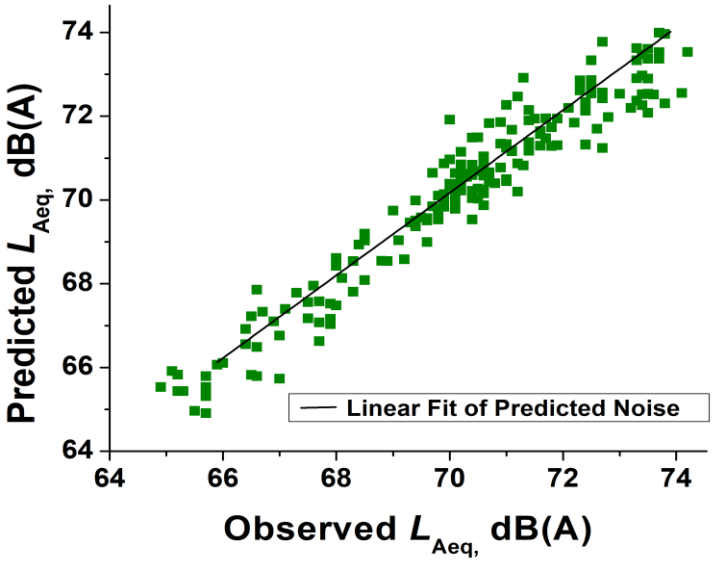

Figure 6.8. Training performance of L_{eq} model for experimental data

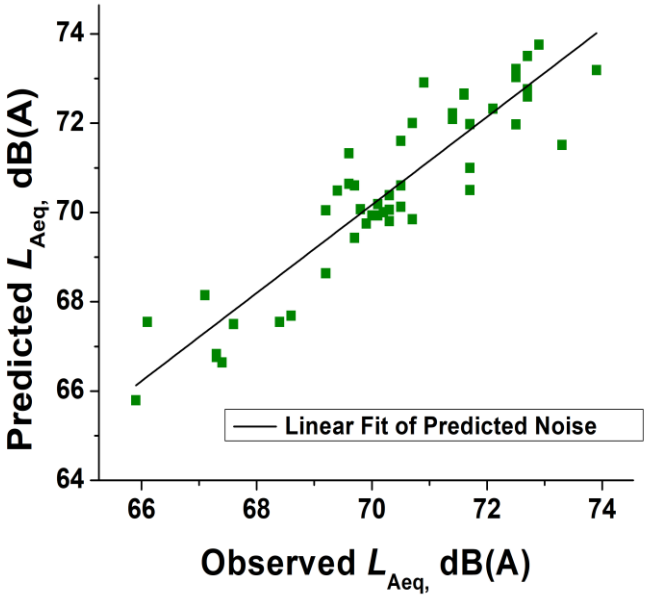

Figure 6.9. Testing performance of L_{eq} model for experimental data

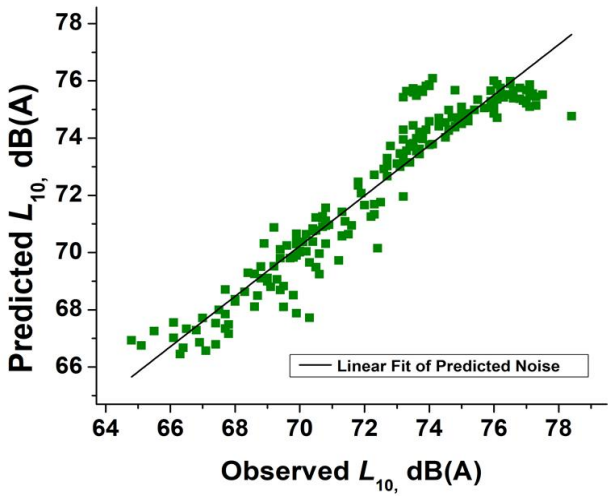

Figure 6.10. Training performance of L_{10} model for experimental data

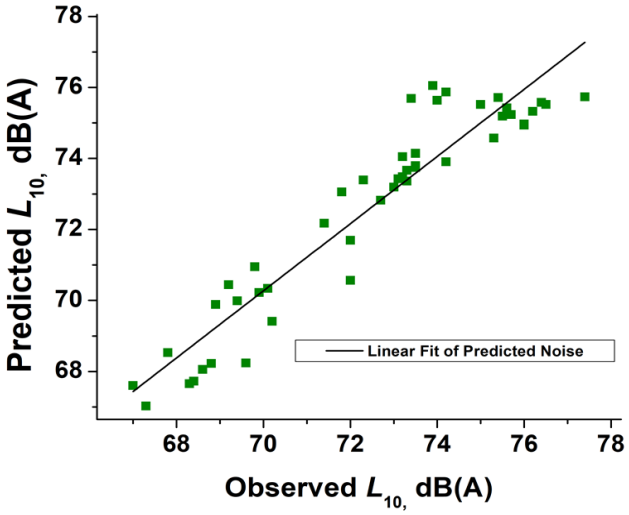

Figure 6.11. Testing performance of L_{10} model for experimental data

Table 6.4. Model results

Performance measurement parameters	L_{eq}		L_{10}	
	TR	**TS**	**TR**	**TS**
R^2	0.9284	0.8389	0.9048	0.8959
R	0.9635	0.9159	0.9512	0.9465
MAE	0.4592	0.6729	0.7237	0.7626
RMSE	0.5948	0.8282	0.9670	0.9232

6.4.6 Garson algorithm

The ANN model may be trained with a wide range of influencing variables, i.e. inputs, improving its predictions' accuracy. To counteract the situation better, knowledge and priority of influencing variable is advantageous. Utilizing the connection weight of the ANN model, the Garson algorithm proposed by [257] and modified by [258] is applied to rank the input variables in order of relevance. Equation (6.4) describes the Garson algorithm. A_{xz} represents the input variable's significance in relation to the other input variables, w denotes the number of neurons, M_{xy} is the connection weight between the input neuron x and the hidden neuron y , O_{yz} is the connection weight between the hidden neuron y and the output neuron z, and $\sum_{Q=1}^{N} |M_{Qy}|$ is the sum of the connection weights between the N input neurons and the hidden neuron y and w denotes the number of neurons. Figure 6.12 shows the input variable's significance in relation to the other input variables. As discussed previously, total 15 number of variables were chosen to model the vehicular traffic noise for high rise buildings. As shown in Figure 6.12 Garson's algorithm approach assigns primary importance to Q1 (2- wheeler

volume) which is 14.07 % followed by Q2 (3 -wheeler volume) (11.99%), HD (Hypotenuse distance from centre (HD) of road) (11.80%), HE (Honking events) (9.59%), Q6 (Rickshaw volume) (7.19 %), Q3 (LCV volume) (7.04 %), Q4 (Bus volume) (6.53%), Q7 (Cycle volume) (5.88 %), Q5 (e-rickshaw volume) (4.26 %), V3 (Car speed) (5.20 %), V2 (3-wheeler speed) (3.48%), V4 (LCV speed) (3.38 %), V1(2 -wheeler speed) (3.34 %), V5 (Bus speed) (3.25 %) ,V6 (Rickshaw speed) (2.91%).

$$A_{xz} = \frac{\sum_{y=1}^{w}(|M_{xy}O_{yz}|/\sum_{Q=1}^{N}|M_{Qy}|)}{\sum_{X=1}^{N}(\sum_{y=1}^{w}(|M_{xy}O_{yz}|/\sum_{Q=1}^{N}|M_{Qy}|)} \quad (6.4)$$

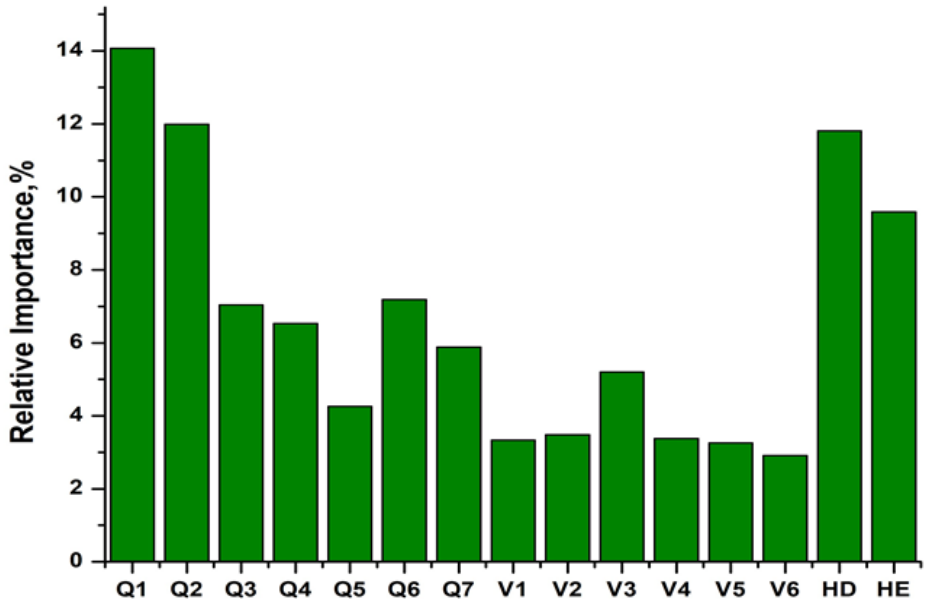

Figure 6.12. Relative importance of input variables

6.5 Discussion

The noise level is expected to decrease with increasing distance [259, 260]. Ground absorption plays an important role in reducing the noise levels. In contrary to this expectation, the measured data show that the noise level values do not decrease with increasing altitude. As the height of building rises, the ground absorption diminishes and eventually disappears. The propagation medium through which environmental noise travels is also an essential factor. Air is believed to be a homogeneous medium through which environmental noise travels. However, air characteristics—like wind speed, temperature, and humidity—change with spatial position and, more specifically, altitude [146]. It was observed earlier that noise level increases with height up to the 3rd floor and then starts to decrease. This peak floor noise level may change from place to place because of different propagation conditions, i.e. free field and reverberant field. The reverberation caused by many reflections of sound waves, elevates the ambient noise level in urban areas. The alternating rise and fall of noise levels along the altitude of high rise building under reverberant field condition may be called the 'canyon effect'. The field condition in this research is reverberant with opposite side buildings 2-3 floor height having similar concrete façade as building 1 and 2 under study. It is known that concrete façade helps reverberation. There were no obstacles between the source and the receiver which permitted the propagation of noise signals to cause canyon effect. So, the result of this research may suit other regions with similar field conditions.

Analysis of the frequency spectrum show that most of the sound energy on each floor of building 1 (33.3 m away from the edge of the nearby carriageway) was caused by low-frequency noise up to 200 Hz. and honking noise at 3.15 kHz. In contrast, most of the sound energy on most of the floors of building 2 (which is 18.4 meters from the edge of the nearby

carriageway) was also by low-frequency noise up to 200 Hz. However, the honking noise at 3.15 kHz. is more prominent due to closer proximity to the source. Traffic noise is reckoned to be low frequency noise as discussed earlier. Noise at low frequencies may also be distracting causing annoyance and dissatisfaction [146], and affect cognitive abilities [261].

TNI serves as a pivotal tool for evaluating how traffic noise impacts architectural designs and urban planning. It sets a standard for the acceptable level of amenity in today's urban environments, with a permissible limit of 74 dB [242, 262] . Notably, building 2, positioned closer to the road, exhibits a notably higher mean TNI and NC value compared to building 1, which is situated further away. For building 2 residential complexes, the mean TNI registers at 78.43, while for Building 1, it stands at 67.6. Building 2 consistently surpasses the permissible TNI limit across all floors from the 1st to the 12th, with particularly elevated levels noted between the 3rd and 10th floors, suggesting lower acoustic comfort in these mid-levels compared to higher floors as shown in the Table 6.1. However, TNI drops below 74 dB beyond the 12th floor. Conversely, building 1 maintains TNI levels within acceptable bounds throughout. Additionally, building 2 exhibits an average NC value of 11.18 dB(A), surpassing building 1's average of 9.3 dB(A). A higher NC value denotes heightened annoyance stemming from sound level fluctuations within specific time intervals [263, 264]. The pronounced disparities in TNI and NC values between building 2 and building 1 underscore the significant impact of building distance from the road on acoustic comfort. This factor warrants careful consideration when formulating mitigation strategies.

In this medium-sized Indian city, a significant portion of the road traffic is generated by two-wheeled vehicles, with estimates ranging from 53 per cent to 69 per cent for Ashapur road and from 63 per cent to 75 per cent for Mahmoorganj -Sigra Road. This two-wheeler volume

significantly contributes to the city's noise pollution. The two-wheeler traffic volume was given the highest ranking in the Garson algorithm's approach as an influential variable compared to the other variables considered for the cause of traffic noise pollution. The poor traffic management of this city, i.e., different and undisciplined driving styles, improper parking, and lack of a systematic pedestrian crossing method, is also responsible for traffic noise pollution. In developing countries; where traffic is more diverse, honking by vehicles is more pronounced [66]. The behavior of drivers in metropolitan areas of developing countries may be the cause of high noise levels, who use their vehicle horns more often than drivers in developed countries [265]. The ineffective management of traffic leads to congestion and honking, both of which contribute to excessive noise, as a result, this city also requires effective control of its traffic to combat noise pollution. The developed models are efficient in predicting the L_{eq} and L_{10} at a different floor at the high-rise residential building for heterogeneous traffic flow conditions in a country like India. However, the developed model is likely to be applicable to similar geo-environmental conditions and heterogeneous traffic in the plain areas. It may however be ensured that there are no obstacles between the source and the receiver, and conditions for reverberant field exists. The wind speeds should be lower than 4 m/s and the weather should be fair. The SLM should be calibrated before use.

6.6 Conclusion

In a country like India, many high–rise buildings are situated less than 50 meters from the road edge. Exposure to traffic noise can cause a variety of health problems. Realizing the scope of the noise issue gives us the motivation to make a significant contribution to the field of noise control after learning about the breadth of the noise problem, and we did it by creating

a model to forecast traffic noise for tall buildings. The most important findings are summed up below:

1. This study demonstrated how noise level changes with altitude in high-rise buildings. The study's findings showed that noise level increases to a maximum up to a certain height before dropping off. The L_{Aeq} level were ranged between 62.9-73.8 dB(A) for building 1 and 69.4 – 74.2 dB(A) for building 2. These L_{Aeq} have surpassed the assigned legislative range of 50-55 dB(A) for India and the similar value of outdoor living area stipulation of the WHO.

2. The finding also revealed that floor levels 3, 4, 5 and 6 were the noisiest in the buildings studied. Therefore, from the perspective of noise, it may be suggested that the 1st floor or any floor above the 10th may afford serene living conditions.

3. Acoustic amenity of lower and middle floors levels is found to be low as compared to higher floors as they have TNI value less than 74 dB(A). The distance of the building from the road plays an essential role in acoustic amenity, which may be a critical factor from a mitigation strategy point of view.

4. Frequency analysis of both buildings show that, when it is closer to the roadway the honking noise dominates over the usual traffic noise. However, when the building is located at a distance of about 30m away, the traffic noise dominates, and the impact of honking noise is comparatively lower.